Identifying and Repairing Catastrophic Errors in Galaxy Properties

Beryl Hovis-Afflerbach [1,2] | Charles Steinhardt [2] | Peter Capak [2,3] | Gabriel Brammer [2]

1 Caltech
2 DAWN
3 IPAC/Caltech

Introduction

Spectroscopy

- Allows for accurate determination of galaxy properties.
- Too expensive for most uses.

Photometry

- Only choice for large surveys.
- Requires template fitting to determine galaxy properties.
  - Usually correct but sometimes catastrophically wrong.

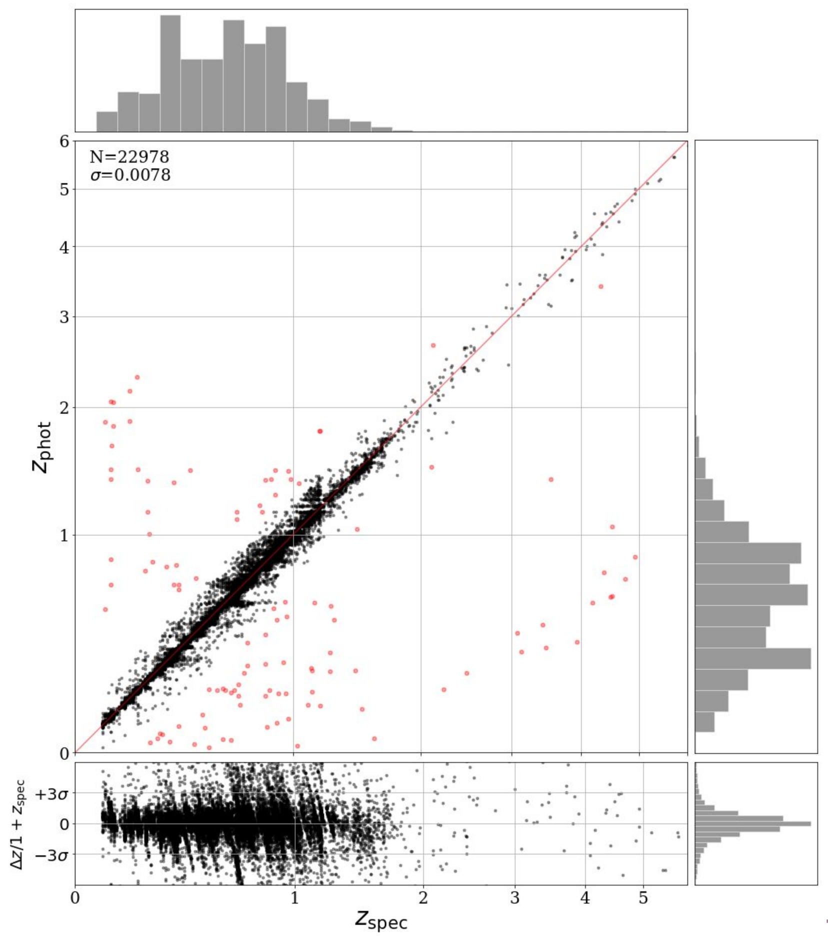

Template fitting codes such as EAZY (Brammer et al. 2008) have high success rates but for a few percent of objects produce **large, systematic errors** (Figure 1).

Figure 1. Redshift used as diagnostic to determine success of EAZY template fit by comparing with spectroscopy. 99.5% of objects (black) fall on or near the y=x line, while the other 0.5% (catastrophic errors, red) have error $\Delta z/(1+z_{spec}) > 0.15$. On plot below, showing distribution of error around the y=x line, the (red) objects with catastrophic errors have errors much greater than ±6σ and do not appear.

Can we identify objects with errors without using spectroscopy? Can we fix these errors and determine the correct properties?

Method

Group similar galaxies

- Problem: galaxies are sparse in 8 dimensions.
- Solution: use dimensionality reduction algorithm (t-SNE, van der Maaten et al. 2008) to **group galaxies with similar photometry in a low dimensional space** (Figure 2).

We run t-SNE on normalized total fluxes at 8 bands (u, r, z++, yHSC, Hw, Ksw, IRAC1, IRAC2) and observe that:

- Grouping objects by SED shape induces a grouping by redshift.
- Objects which stand out in grouping are frequently the objects with catastrophic errors we seek to identify.

Compare redshift with near neighbors

- We take the mean photometric redshift of all objects within some radius of an object (excluding that object), and compare this mean with the photometric redshift of the object itself (Figure 4).
- We flag those for which $|z_{phot} - z_{mean}|$ > **threshold** as the group predicted to have catastrophic errors in photometric redshift.

This method correctly identifies objects with catastrophic errors at a higher rate than it mistakenly flags objects without (Figure 5).

Results

Figure 2. t-SNE output with 5000 iterations and perplexity 35, colored by photometric redshift. For a few groups of objects, the SED shape is shown at left. Objects grouped close together have similar SED shapes.

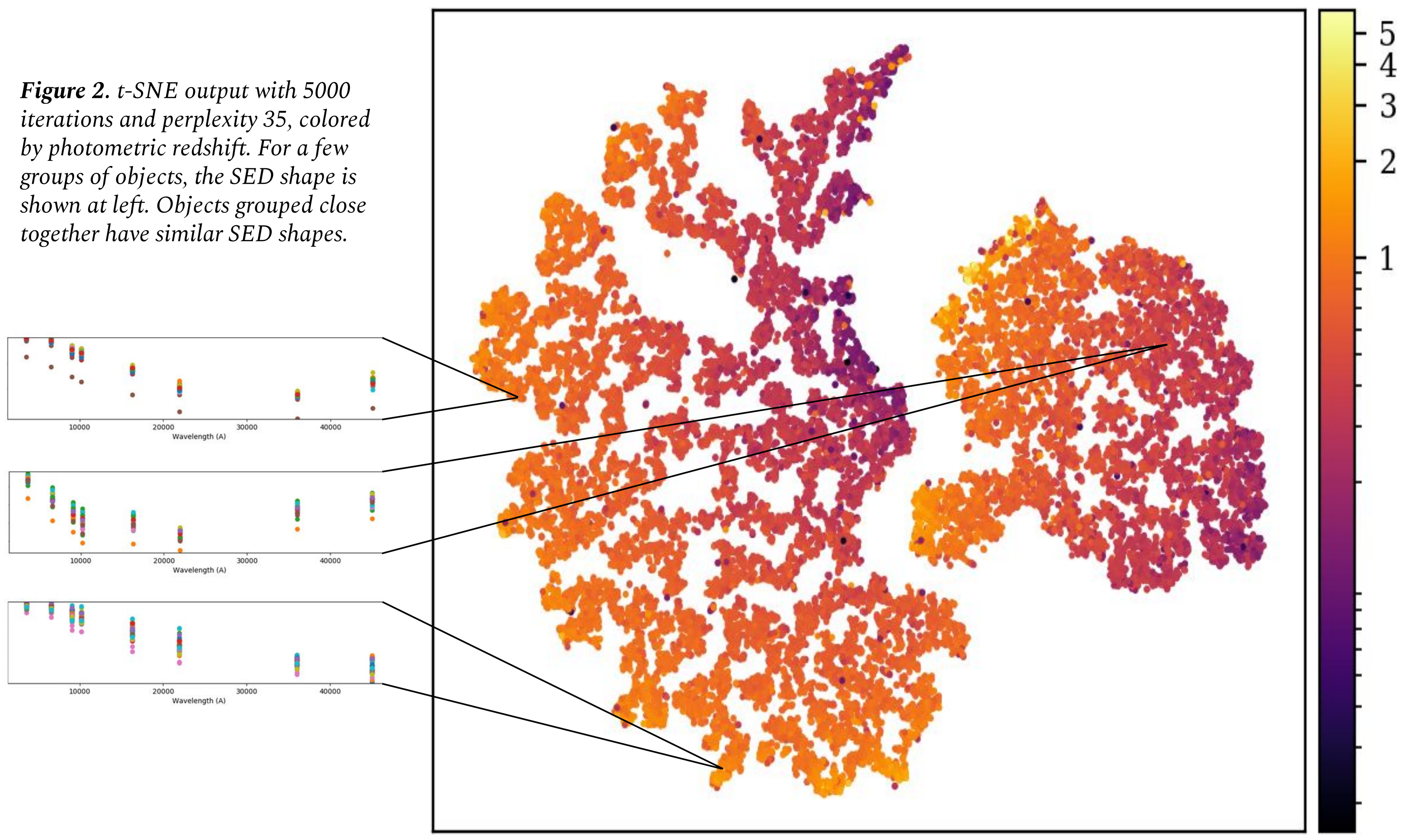

Neighbor comparison

Figure 3. The same t-SNE map (5000 iterations, perplexity 35) colored with catastrophic errors in red. Many of the points where the photometric redshift is different than that of the objects around it (color stands out in Figure 2) are also objects with catastrophic errors (red points in this figure).

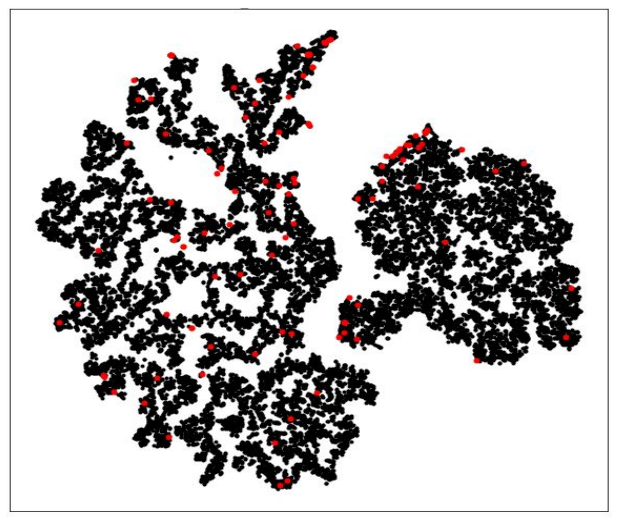

Figure 4. Comparison of photometric redshift of each object with the mean photometric redshift of neighboring objects in t-SNE output, for randomly chosen control sample of 111 objects (a) and for the 111 objects with known catastrophic errors (b).

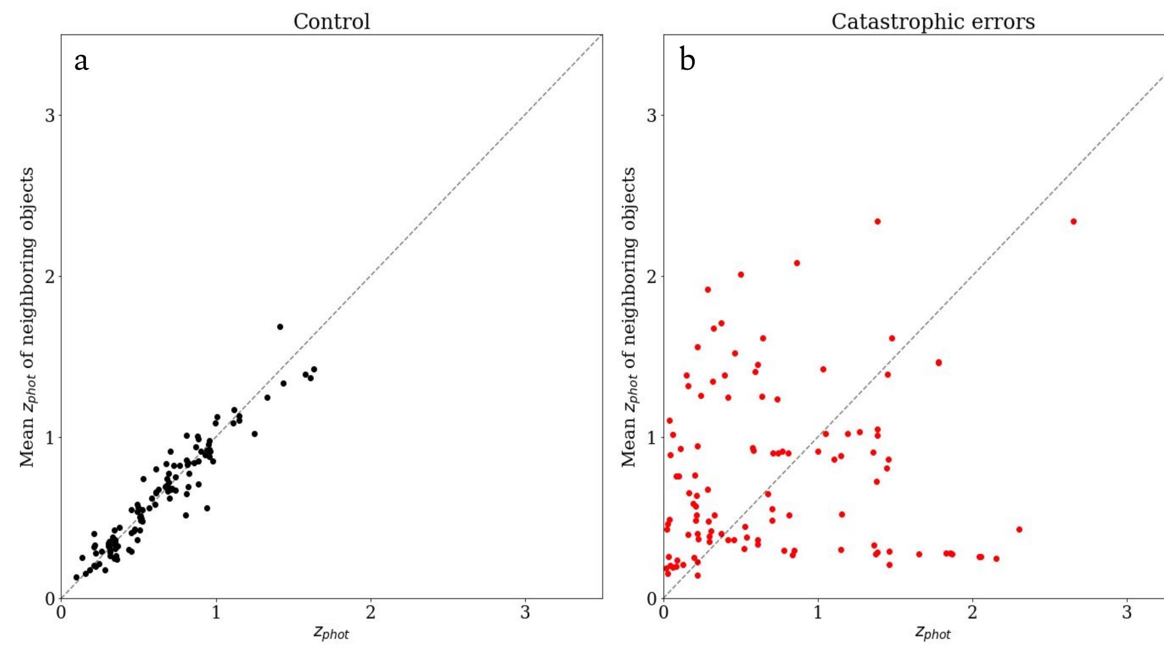

ROC curve

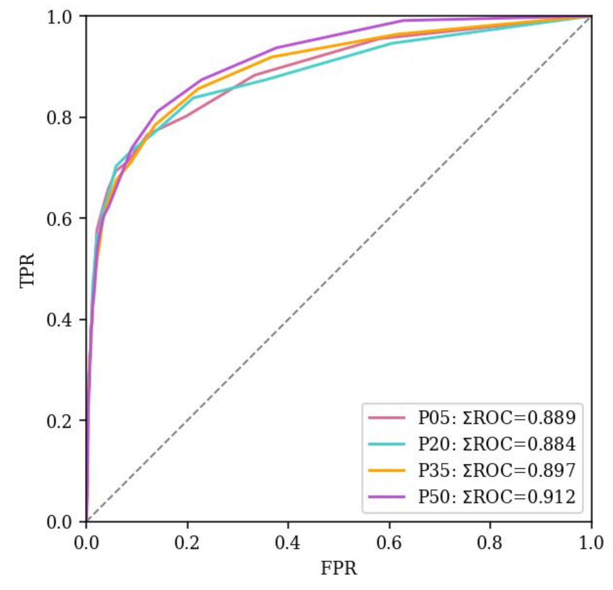

Figure 5. Receiver operating characteristic (ROC) curve for method of flagging an object if its photometric redshift differs from the mean of its neighbors by at least some threshold, with four different values of perplexity.

For each threshold, we plot the true positive rate at which we correctly flag catastrophic errors against the false positive rate at which we identify correct objects as errors.

Since this curve lies far above the dashed line (would be comparable to guessing randomly) and has an integral (ΣROC) closer to 1 than to 0.5, this method consistently correctly identifies errors at a much higher rate than it misidentifies correct objects as errors.

Perplexity

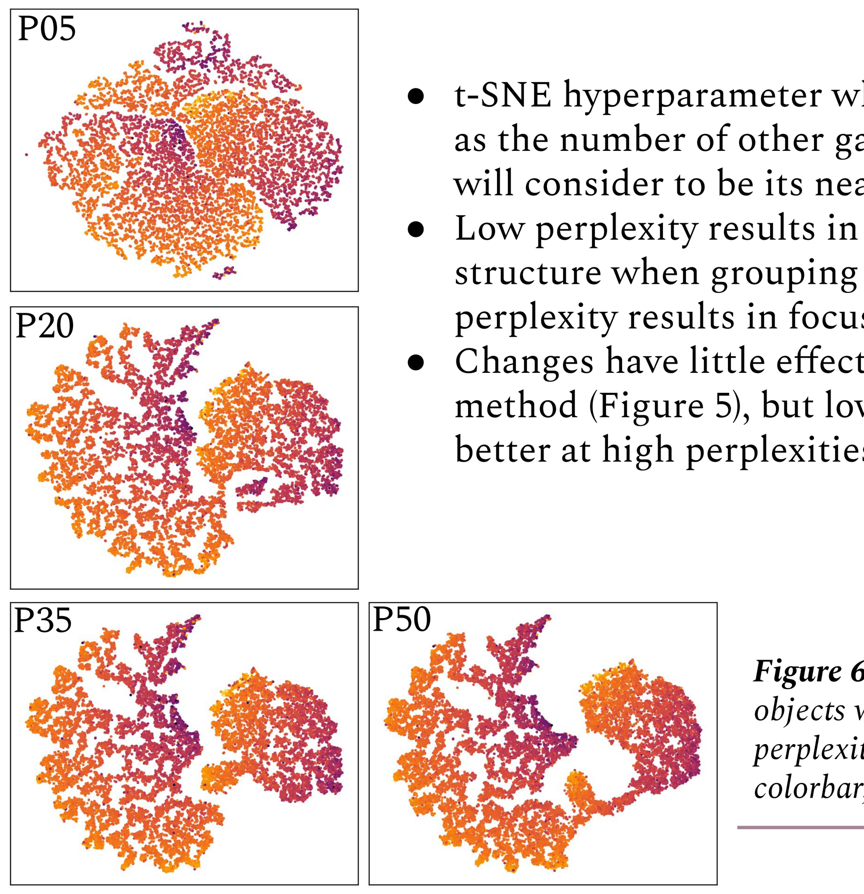

- t-SNE hyperparameter which can be interpreted as the number of other galaxies that each galaxy will consider to be its nearest neighbor.
- Low perplexity results in focus on local structure when grouping objects, and high perplexity results in focus on global structure.
- Changes have little effect on performance of method (Figure 5), but low thresholds perform better at high perplexities and vice versa.

Figure 6. t-SNE output for all objects with 5000 iterations and perplexities 5, 20, 35, and 50. (For colorbar, see Figure 2).

Attempts to Repair Errors

We have identified objects with catastrophic errors. Can we determine their correct properties?

NO.

We have tried:

1. Replacing the redshift of each flagged object with the mean photometric redshift of its neighbors (Figure 7).
2. Rerunning EAZY on flagged objects with a 10 or 100 times finer redshift grid.

Both methods introduce more error than they eliminate, giving us a set of objects which have similar properties to their neighbors but fail template fitting.

These are interesting objects which we should investigate further.

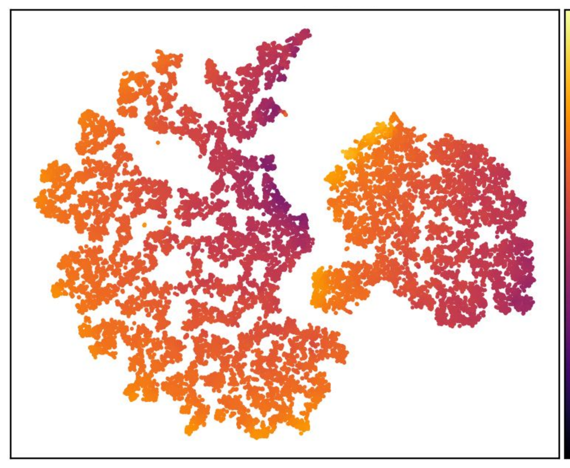

Figure 7. The same t-SNE map with perplexity 35 but each object is colored by the mean z_{phot} of its neighbors.

Conclusions

- A t-SNE grouping by SED shape allows us to identify majority of objects with error $\Delta z/(1+z) > 0.15$ without the use of spectroscopy.
- It is a versatile method and can be used to eliminate some objects with errors with little effect on the rest of the sample, or to eliminate as much error as possible while still preserving a usable portion of the sample.
- We have found no reliable way to determine the correct properties but have identified an interesting set of galaxies to investigate.

Future Work

- Explore other correction methods.
- Further investigate correlations to properties other than photometric redshift for objects with errors.
- Investigate effects of adding more bands for t-SNE grouping (but smaller N since t-SNE is unable to work with incomplete data).

References

Brammer, G. B., van Dokkum, P. G., & Coppi, P. 2008, ApJ, 686, 1503, doi: 10.1086/591786
Hemmati, S., Capak, P., Pourrahmani, M., et al. 2019, ApJ, 881, L14, doi: 10.3847/2041-8213/ab3418
Hildebrandt, H., Arnouts, S., Capak, P., et al. 2010, A&A, 523, A31, doi: 10.1051/0004-6361/201014885
Jin, S., Daddi, E., Liu, D., et al. 2018, ApJ, 864, 56, doi: 10.3847/1538-4357/aad4af
Laigle, C., McCracken, H. J., Ilbert, O., et al. 2016, ApJS, 224, 24, doi: 10.3847/0067-0049/224/2/24
Masters, D., Capak, P., Stern, D., et al. 2015, ApJ, 813, 53, doi: 10.1088/0004-637x/813/1/53
Speagle, J. S., & Eisenstein, D. J. 2017, MNRAS, 469, 1186, doi: 10.1093/mnras/stw1485
van der Maaten, L. 2014, JMLR, 15, 3221.
van der Maaten, L., & Hinton, G. 2008, JMLR, 9, 2579.

Acknowledgements

Thank you to Kathryn McEachern for your generous contribution to the SURF program and to this research in memory of David L. Glackin.

Based on data products from observations made with ESO Telescopes at the La Silla Paranal Observatory under ESO programme ID 179.A-2005 and on data products produced by TERAPIX and the Cambridge Astronomy Survey Unit on behalf of the UltraVISTA consortium.